Defence Science Journal, Vol. 65, No. 5, September 2015, pp. 367-371, DOI : 10.14429/dsj.65.8714

94 GHz Radiometer for Benchmarking its Operational Parameters for the Remote Detecton of Concealed Threat

Ashok Kumar[*,!] and B.S. Jassal[#]

[*]*Defence Electonics Applications Laboratory, Dehradun - 248 002, India*
[#]*Grapic Era University, Dehradun -248 002, India*
[!]*E-mail: akumarkalra@yahoo.co.in*

ABSTRACT

Standoff detection of concealed threat, using millimeter wave radiometer, is being experimented worldwide for enhancing the frame rate and detection probability, as an alternative to personnel frisking, for enhancing passenger service rate and avoiding exposure to harmful radiations. The development of 94 GHz Dicke radiometer and experimentation to bench mark its operational parameters like spatial sampling rate, scan rate and dwell time for the detection of concealed threat, under the fabrics of a human is described. The experimentation provided operational methodology and imaging phenomenology in a given background for the detection of metallic threats. The experimental results have established that radiometer can be considered as an alternate to frisking of personnel and celebrities at public places for security reasons.

Keywords: Radiometer, millimeter wave, cosmic noise, imaging technology, remote detecton

1. INTRODUCTION

Millimeter wave imaging technology has emerged as an alternative to infrared (IR) and visible band for all weather security and surveillance operations needed for home land security due to its ability to provide 200 times[1] more contrast compared to IR counterpart. Due to this property, radiometer sensors can 'detect' concealed threats, embedded on the body of human, from standoff distances. In this process outline of the anatomy of the body is also displayed to the operator, which has been always a conflict between security system and potential threat carriers on the pretext of privacy invasion. However public has now become more aware and is ready to compromise its privacy for getting better security services.

The basic principle underlying the detection of concealed threat is the measurement of antenna temperature contrast i.e. antenna temperature variation between threat and the background. This contrast appears as voltage variation when radiometer scans a potential area of probable threat. The voltage level from the radiometer corresponds to the properties of the object present in the beam and standoff distances. Properties of the object include its material, shape, size, orientation, background, fabrics layer and weather conditions. The DC voltages received from the radiometer, as a function of antenna positions, are plotted in grey levels between black and white as a function of angular position. Metallic threats with almost zero emissivity (100 per cent reflectivity) are plotted as white, however higher emissivity objects like vegetation, human body are plotted as grey shade.

Extensive experimentations have been conducted for optimising operational parameters of the radiometer to finalise scan rate (°/s), spatial sampling rate (no. of samples per antenna beamwidth in both orthogonal directions), integration time (ms) and angular scan limits. Image data collected has shown that metallic threat concealed on the human body can be detected or missed depends on operational parameters of the sensor. The detection process becomes more challenging with dielectric threat, due to its poor contrast from the embedded background. This poor contrast between the dielectric threat and human body, further deteriorate below the thermal resolution of the radiometer, due to attenuation of the concealing fabrics and intervening atmosphere between the imaging sensor and the threat.

During the experimentation process a metallic object was concealed under the fabrics of a human and radiometer was programmed to scan an area around the human body with and without concealed metallic object in raster manner. The DC output of the radiometer was plotted as an image on grey scale. A white blob was visible at the place of metallic threat. DC voltages were taken from one of the horizontal rows of the image, passing through the blob and plotted as a function of angular scan angle in horizontal direction with and without metallic objects. The enhancement of voltage along the x-axis, at the spot of blob indicated the presence of metallic object, proving the possibility of detection of concealed threat.

Received 08 May 2015, revised 03 August 2015, online published 08 September 2015

2. UNDERLYING DETECTION PRINCIPAL

Jing-hui[2] and Samluk[3] have explained the utility of Planck's black body radiation for radiometric imaging sensor. According to this law, spectral brightness of the blackbody increases with the temperature. An important approximation to Planck's blackbody radiation law is the Rayleigh-Jeans law, which states that the spectral brightness at 94 GHz is very low compared to IR, due to which very low energy is available for operating radiometers for security surveillance. However there is increased interest in research of radiometer sensor for concealed object detection, because of the fact that available energy is enough for the detection of threat with higher reliability due to large contrast of reflective metallic threat, embedded in higher emissive background. At millimeter wave frequencies human body has an emissivity near unity while that of metallic threat is of the order of 0 to 0.2. This low value of emissivity (or high value of reflectivity) reflects cold cosmic noise for the generation of required contrast in the background of human body. During experimentation on radiometer, large variations in brightness temperature were observed when antenna beam crossed the concealed metallic object. This variation helped discerning the metallic threats in high emissive background.

The radiation flux density received by the antenna of the radiometer sensor is measured in power (dBm) units and is related to the object and atmosphere parameters as[4,5]

$$R_{\sum} = K(T_{object} + T_{ref.sky} + T_{background})B_n \quad (1)$$

where, T_{object} is the emission from the object in the main beam of the antenna. It is the product of object temperature with its emissivity, multiplied by beam fill factor and reduced by atmospheric attenuation. $T_{ref.sky}$ is the reflected cosmic noise from the metallic targets. It is the product of radiometric cosmic noise temperature with reflectivity of the object and antenna beam fill factor and reduced by atmospheric attenuation. $T_{background}$ is the emission noise of the background in which metallic object is immersed. This flux corrupts the useful signal received from the object. It is the sum of physical temperature of the background multiplied by its emissivity. This whole flux is multiplied by the beam fill factor excluding the area occupied by the target. This value is again reduced by the atmospheric attenuation. K is Boltzmann's constant, and B_n is noise bandwidth of the radiometer.

The total flux received from the scene in the main antenna beam gets corrupted by the flux received from the side lobes of the antenna. The contribution of the flux from the main and side lobe is given by

$$R_{\sum} = K\{(\eta T_{main\ lobe} + (1-\eta)T_{side\ lobe}\}B_n \quad (2)$$

where η is the antenna beam efficiency, $T_{mainlobe}$ is the flux received through the main lobe and $T_{sidelobes}$ is the side lobe contribution. Offset reflector antenna with 500 mm aperture and 0.4° beam width has been designed for the realisation of the radiometer sensor. Its beam efficiency was more than 90 per cent, therefore error in the measurement of contrast temperature between background and threat, due to side lobe was below 10 per cent.

3. DESCRIPTION OF THE SENSOR

A 94 GHz imaging sensor with programmable positioning system and scan controller has been designed, developed and realised to conduct experiments for exploring feasibility of detection of concealed threat from standoff distances. It contains a Dicke type radiometer, offset reflector antenna, data acquisition system and a display for the concurrent visualisation of the received data as shown in block diagram Fig. 1. Selection of 94 GHz frequency of operation of the sensor is an optimum tradeoff between spatial and thermal resolution with manageable antenna size and millimeter wave component technology constraints. The dicke type configuration of the radiometer provides stable operation, through inbuilt periodic calibrations. It has thermal sensitivity of the order of 0.05 K@1 s integration time, system noise temperature 900 K and pre detection bandwidth 4000 MHz.

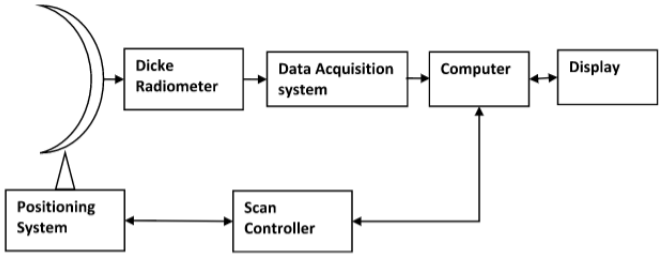

Figure 1. Block Diagram of 94 GHz Imaging Sensor.

Calibration of the radiometer was carried out by feeding the noise power, equivalent to noise temperature 100 K - 332 K with the help of controllable liquid nitrogen loads. The calibration data between input noise temperature and output voltage, using liquid nitrogen loaded calibrated Dewar, provided a transfer slope of 15 mv/K. Fig. 2 shows the realised radiometer sensor test setup for experimentation.

Figure 2. Radiometer sensor test setup.

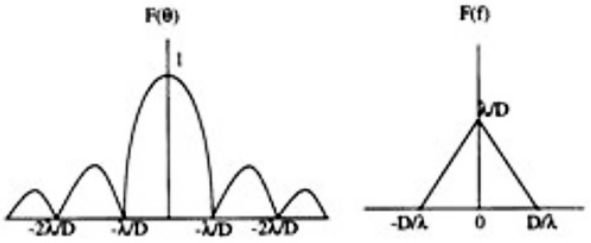

Figure 3. Antenna power pattern and its frequency spectral function.

4. OPERATIONAL PARAMETERS OF THE SENSOR

The fundamental information that radiometer sensor detects is the antenna temperature contrast ΔTc, between the two conditions, when there is target (metal) on the human body and when there is no target on the human body. The antenna scans in two co-ordinates i.e. in raster manner. After the antenna has scanned from left to right, the elevation angle is changed according to command and antenna moves back from right to left. The procedure is repeated until the whole region is scanned.

The scanning speed and data pick up steps of the sensor are related to the radiometer parameters i.e. integration time leading to thermal sensitivity and antenna beam width. Every antenna acts as a low pass filter, in the spatial domain, and attenuates sharp features (high frequency components) of the scene. As per antenna response shown in Fig. 3 sensor will attenuate signals corresponding to brightness temperature if spatial frequency of the scene is greater than |D/λ|. According to sampling theory, all the signals whose spatial frequencies are <D/λ can be sampled for detection. The sampling frequency must be at least twice the spatial frequency i.e.

$$f_s \geq \frac{2D}{\lambda} \tag{3}$$

Sampling spatial interval is

$$\theta_s = \frac{1}{f_s} \leq \frac{\lambda}{2D} \sim= \frac{\theta_{3dB}}{2} \tag{4}$$

where θ_{3dB} is the Beam width of the antenna.

This shows that at least 2 samples per beam width are essential to acquire the scene having spatial frequency corresponding to D/λ. Therefore large aperture or lower wavelength antenna acquires higher spatial frequencies of the scene resulting in better quality of the imager. To fully exploit the sensitivity of the radiometer, sampling interval (antenna dwell time on each step) must be equal or greater than the integration time of the radiometer. For the finalisation of the operational parameters of the radiometer sensor integration time, spatial sampling interval and scanning speed are iterated experimentally for the extraction of higher frequency features of the scene taking into consideration the latency of the data acquisition system. After lot of iteration and image data interpretation, operational parameters finalised are 4°/s scan speed with registering two pixels per beam width along with integration time of 30 ms per pixel.

5. THEORETICAL EXPLANATION TO THE EXPERIMENTATION

In the experimentation of data collection with optimised parameter of the sensor, contrast in the scene is considered for detection. As indicated in Fig. 4 upper part of the body reflects cold sky radiation predominantly, while lower body reflects warm ground radiation, resulting in large variation of brightness temperature on background. An object concealed under the fabrics, must have different emissivity compared to the skin for contrast generation. With different emissivity, the object will not only block the emissive radiation of the background, but also reflect the cold sky noise, resulting in high contrast as indicated in Fig. 4. Contrast of the metallic threat concealed on human body is calculated by assuming body[6] temperature as 310 K.

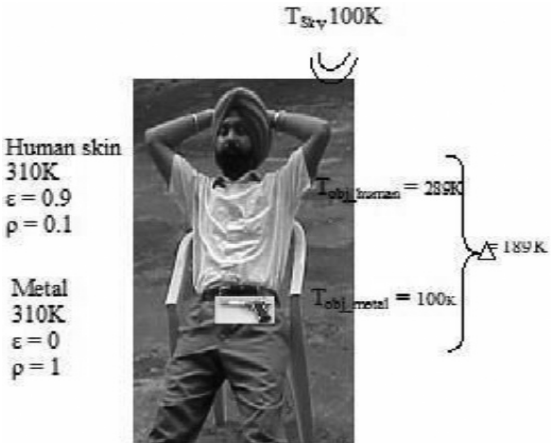

Figure 4. High Contrast of metallic object concealed on human body.

Brightness temperature of the body in outdoor scenario is

$$T_{obj\_human} = 310 \times 0.9 + 100 \times 0.1 = 289K$$

where 310 K is the temp of the human body and 0.9 is its emissivity. 100 K is the equivalent noise temperature of the sky noise illuminating the body and 0.1 is its reflectivity.

Similarly Brightness temperature of the metallic object in outdoor scenario is

$$T_{obj\_metal} = 310 \times 0 + 100 \times 1 = 100K$$

Contrast between background and concealed threat is 289-100 = 189K in the target plane, which gets lower in the detection plane due to range, antenna efficiency and system noise temperature.

6. EXPERIMENTATION AND RESULTS

A man with and without a metallic threat under his shirt and pocket sitting on a chair has been scanned in two planes in a raster fashion measuring ±15° in azimuth and ± 12.5° in elevation. The man was sitting at about 8 meters from the sensor and the sensor was programmed to scan at 4°/s speed for data acquisition. The data was registered every 0.2° in both planes within a span of 30° azimuth and 25° elevation resulting in 150 x 125 pixel data. The acquired data from the radiometer as a function of angular position is fed to the ADC and counts are plotted in azimuth-elevation plane. The plots are converted to jpeg format for display. Two sets of experiments

were performed, one with a metallic gun hidden on the left side of chest and another with a metallic gun hidden inside the left pocket of trouser. Figures 5(a) and (b) show the image of man without and with metallic object under his fabrics respectively. Figure 5(c) indicates graphical display of data taken from two images with same row location. X-axis indicates no of points registered at every 0.2° in a total span of 30°. Y-axis indicates ADC counts corresponding to the amplitude received at its input. Input to the 10 bit ADC from radiometer has been conditioned between 1.7 V - 5 V corresponding to 100 K-332 K brightness temperature of the scene after referencing with standard load of 333 K as per Dicke radiometer principal. 1.7 V corresponds to 1062 counts whereas 5.0 V gives 2048 counts. The difference in the signal level between two plots in Fig. 5(c) is of 100 counts which correspond to 12 K enhancement in brightness temperature due the presence of the metallic threat. Similarly Figs. 6(a), 6(b), and 6(c) also indicate contrast more than 300 counts, which corresponds to 32 K enhancement over background due to threat.

7. DISCUSSION

Plot at Fig. 5(c) indicates lower contrast (~12 K) between signal without and with metallic threat. This is due to higher cosmic noise reflection from the background (outer bulge of

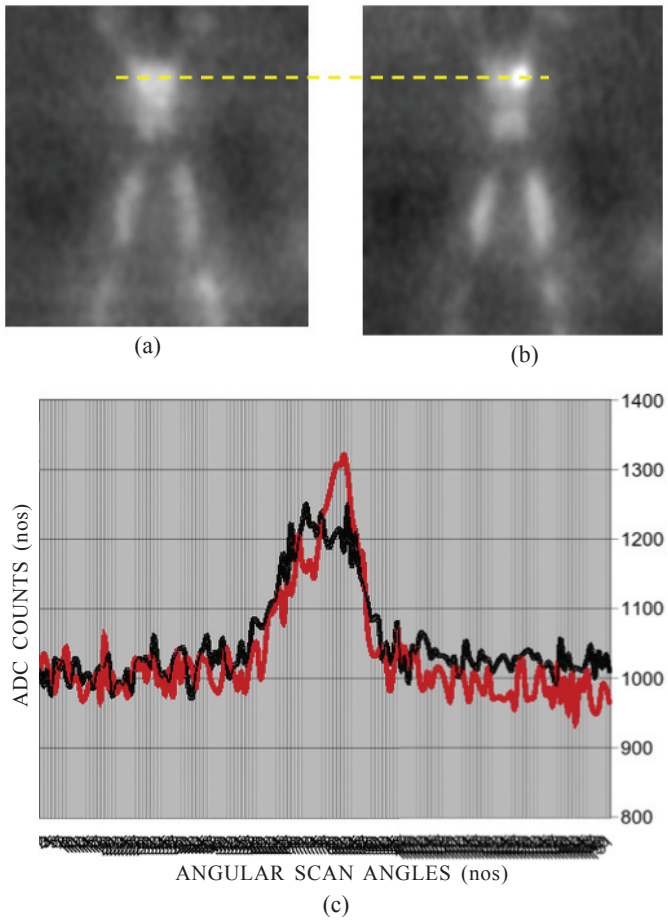

Figure 5. (a) Image of a human without concealed object, (b) Image of a human with concealed object on left pocket, and (c) Signal enhancement due to concealed object.

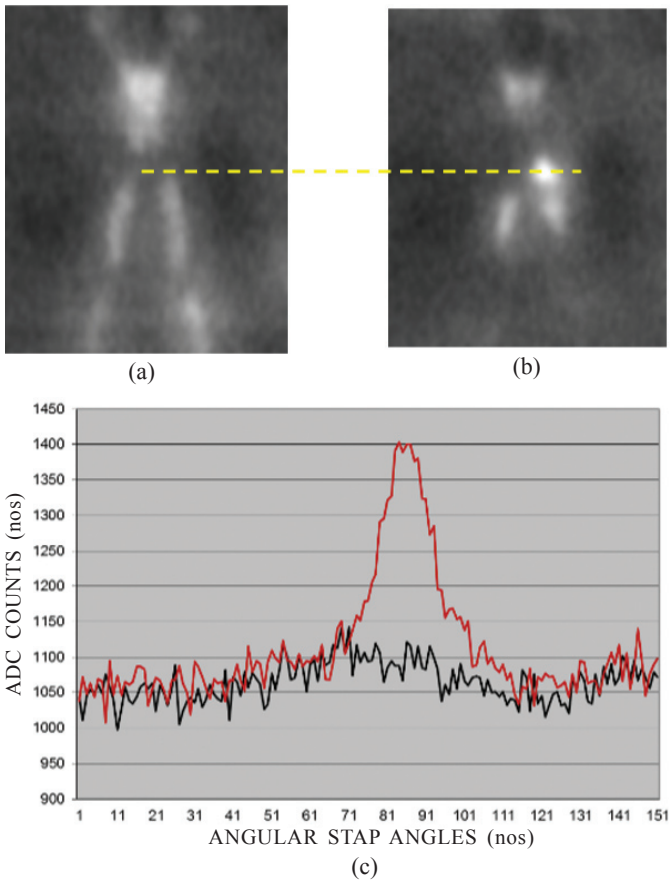

Figure 6. (a) Image of a human without concealed object, (b) Image of a human with concealed object on left trouser pocket, and (c) Signal enhancement due to concealed object.

the chest of the human). In this situation background signal predominates due to cosmic noise reflection from the slant shape of the chest helping large reflection, whereas in Fig. 6(c) background is depressed, in this situation signal received by the sensor from background has no contribution of the cosmic noise reflection. Higher emissive human skin radiated hot noise signal and metallic object reflected cold cosmic noise, resulting in contrast of the order of 32 K. Same metallic threat concealed in different parts of the body, oriented differently may result in different contrast. Large data collection and analysis is necessary for enhancing security effectiveness with reliability.

8. CONCLUSION

Experimentation on 94 GHz radiometer sensor has helped to finalise its operational parameters for data collection. Initial level of data collection has been carried out to analyse signal enhancement due to presence of potential threat. Further experimentation is proposed to add polarisation parameters for enhancing the detection probability.

REFERENCES

1. Appleby, R. & Lettington, A.H. Passive millimeter wave imaging. *Electron. Commun. Eng. J.*, 1991, pp. 13-16.
2. Qiu, Jing-hui; Wang, Nan-nan & Deng, Wei-bo. Research

on millimeter-wave radiometer detection system. *In* IEEE 2008, 2nd International Symposium on Systems and Control in Aerospace and Astronautics, 2008. doi: 10.1109/ISSCAA.2008.4776336

3. Samluk, J.P. Far field millimeter-wave imaging via optical upconversion. Far field millimeter-wave imaging via optical upconversion, Proceedings of SPIE, 0277-786X,V.6948,2008. doi: 10.1117/12.778336
4. Smith, R.M.; Trott, K.D. & Even, Doc. Passive millimeter-wave imaging technology and phenomenology. SPIE, 2558, pp. 390-401. doi: 10.1117/12.2242295.
5. Wilson, W.J.; R.J. Howard & Ibbot, A.C. Millimeter-wave imaging sensor. *IEEE Trans. MTT*, **34**(10), 1026-1035, 1986. doi: 10.1109/TMTT.1986. 1133492.
6. Sato, Masaru & Mizuno, Koji. Millimeter wave imaging sensor. Intechopen, March 2010. doi: 10.5772/9059

ACKNOWLEDGEMENT

We thank Mr H.S. Kalsi for his patient modelling during image acquisition and also his expertise in fabrication and testing of synchronous detector card. We are indebted to Director DEAL for granting permission to publish this experimental work.

CONTRIBUTORS

Mr Ashok Kumar received his MTech (Radar & Communication) from IIT Delhi, in 1990. He is working as scientist 'G' in Defence Electronics Applications Lab., Dehradun since 1986. He has contributed in the development of millimeter wave seekers, passive millimeter wave imaging, 20/30 GHz satcom systems, 38 GHz combat IFF system for combat platforms and troposcatter communication system. He is also carrying out research in blue green laser communication technology for submarine applications. He has authored/coauthored more than 40 research publications. He has designed and realised a 94 GHz radiometer imaging sensor, carried out calibration with hot and cold load and performed experimentations for the optimisation of the parameters for converting it in a product form.

Dr B.S. Jassal received his BSc from Agra University, in 1966; MSc (Physics) from Meerut University, in 1968, and PhD (VHF/UHF propagation) from Jadavpur University, Kolkata, in 1990. He worked in Defence Electronics Applications Lab., Dehradun during 1969 to 2007. In DEAL he headed various research projects relating to RF and Microwave communication, Radiometric studies of atmosphere, terminal guidance systems, satellite communication. Presently he is working in Graphic Era University, Dehradun as Dean, Projects & Consultancy. He has authored/coauthored more than 20 research publications. He helped in enhancing the detection probability and frame rate so that system can be produced for utilisation by the security forces.